Bremsstrahlung linear polarization at incident electron energies of 0.5–1.5 MeV

W. Lichtenberg, A. Przybylski, and M. Scheer
Physikalisches Institut der Universität, D-87 Würzburg, West Germany
(Received 18 June 1974)

At incident electron energies of 0.5–1.5 MeV, bremsstrahlung linear polarization was measured for thin targets of beryllium, aluminum, silver, and gold at emission angles of 10°–122° as a function of photon energy. Data were corrected for electron scattering in the target and for multiple scattering of photons in the Compton polarimeter used. For low-atomic-number targets the experimental results are perfectly in agreement with Born-approximation theory and with computations using Sommerfeld-Maue eigenfunctions, whereas the high-atomic-number results are described satisfactorily only by partial-wave calculations.

I. INTRODUCTION

Calculating atomic-field bremsstrahlung beyond Born-approximation theory (Bethe-Heitler formula[1]) is tedious unless the incident electron energy is restricted to the nonrelativistic (Kirkpatrick and Wiedmann[2]) or extremely relativistic case (Olsen and Maximon[3]). Some early experiments at intermediate electron energies (Motz and Placious[4]) indicate that Born-approximation calculations are poor in this energy range for high atomic number Z of the target.

Calculations at a higher level performed during recent years (Elwert and Haug,[5,6] Tseng and Pratt[7,8]) could not yet properly be checked because of the incompleteness of the former experimental data and because of the large errors involved. Therefore new experiments were carried out to get a more complete (target atomic numbers 4, 13, 47, 79; photon emission angles 10°–122°) and more precise insight into bremsstrahlung polarization at intermediate electron energies (0.5–1.5 MeV).

In the design of the experiments and in data analysis particular attention was paid to all depolarizing effects. Background radiation by scattered electrons was suppressed by a special target-chamber arrangement. To avoid errors due to changing target conditions and to mistakes in beam-current integration both scattering components were recorded by the Compton polarimeter simultaneously. The effect of elastic electron scattering in the target was quantitatively eliminated, and the polarimeter properties were considered including multiple scattering of photons.

The polarization observed depends on (a) kinetic energy T_1 of the incident electrons, (b) atomic number Z of the target, (c) photon emission angle θ, and (d) photon energy k, usually described in units of the maximum photon energy ($\equiv T_1$). The degree of linear polarization is defined by

$$P(T_1, Z, \theta, k/T_1) = (d^2\sigma_\perp - d^2\sigma_\parallel)/(d^2\sigma_\perp + d^2\sigma_\parallel),$$

where $d^2\sigma_\perp$ and $d^2\sigma_\parallel$ denote the cross sections for the bremsstrahlung components with polarization parallel or perpendicular to the reaction plane which contains the directions of both the incident electron and the photon. The cross sections are differential in photon emission angle and photon energy; it is assumed that the incident electrons are not polarized and that the final electrons are not observed.

II. EXPERIMENTAL ARRANGEMENT

Essential parts of the apparatus were built by Järisch[9] and Nowak,[10] who also performed preliminary measurements. A schematic view of the experimental arrangement is shown in Fig. 1. Electrons from a van de Graaff-type accelerator are momentum analyzed by a 45°-sector magnet and a vertical slit (relative accuracy in electron energy better than 3×10^{-3}). The electrons then pass a beam chopper (as a current monitor) and a bending magnet which provides another 45° deflection. All electrons scattered with energy loss by the slit and by the monitor are thus eliminated from the beam.

In the scattering chamber the electrons are extracted upward from the reaction plane by a specially arranged magnet after having passed the target (Fig. 2). Thus measurements at small photon-emission angles are made possible, and bremsstrahlung production at the chamber walls seen by the polarimeter is suppressed. In order to establish that the electrons pass the target horizontally, the beam is directed (by a further magnet) downward for about 7° before entering the scattering chamber. The focus spot has a diameter of about 1 mm, fixed within ±1 mm (vertically) or ±2 mm (horizontally) in the target plane. Beam current was 10–40 μA. The beam was normal to the target except for the emission angle $\theta = 90°$, where the target normal and the beam included an angle of 30°. The targets were prepared by vacuum deposi-

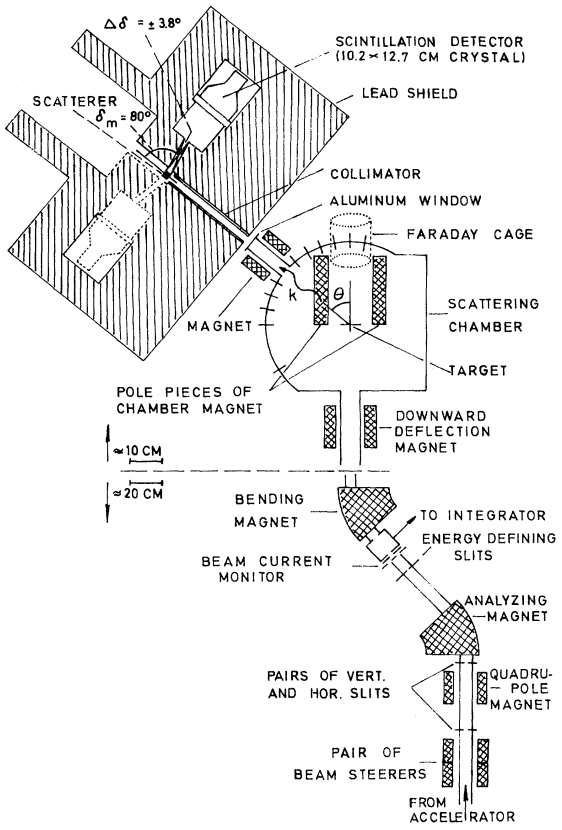

FIG. 1. Beam line with scattering chamber and Compton polarimeter (schematic, seen from above).

tion onto pioloform substrates (≈10 μg/cm^2 thick); in the case of aluminum, commercial foils could be used. In the selection of target thickness (between 250 μg/cm^2 for small θ and high Z and 8.1 mg/cm^2 for large θ and low Z) the effects of elastic electron scattering (see Sec. III B) were taken into consideration.

The bremsstrahlung leaves the scattering chamber through an aluminum window 0.3 mm thick. To be perfectly sure that no bremsstrahlung was produced in the window by scattered electrons, a deflection magnet was applied to the tube to which

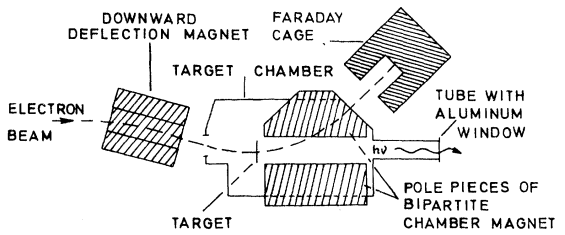

FIG. 2. Downward deflection magnet, scattering chamber, and Faraday cage (longitudinal section, schematic).

the window is mounted (Fig. 1); in addition, background radiation was checked by inserting scattering foils into the electron beam outside the field of view of the polarimeter.

The polarimeter was installed on a table which was rotated around the center of the scattering chamber; Fig. 1 includes a longitudinal section of the polarimeter.

The polarization sensitivity of the polarimeter is based on the fact that Compton scattering of linearly polarized photons is azimuthally anisotropic; the polarization sensitivity depends on bremsstrahlung photon energy k and on scattering angle δ. To obtain a good polarization sensitivity over the whole range of photon energies pertinent here (50 keV $\leq k \leq$ 1.5 MeV) a mean scattering angle $\delta_m = 80°$ was chosen. The angular spread $\Delta\delta$ of the detector slits is ±3.8°. The distance from the target to the scatterer is 725 mm, the length of the collimator is 313 mm, and the inner diameter of its brass insert is 9 mm.

Figure 3 presents polarimeter sections perpendicular to the direction of the incident photons. $D_\parallel$ and $D_\perp$ are 10.2×12.7-cm NaI(Tl) scintillation detectors; S is the cylindrical aluminum scatterer (thickness 3.75 mm, diameter 8 mm). The spread in azimuthal angle $\Delta\varphi$ is ±24.5°; the distance of the detectors from the polarimeter axis is 75 mm. The detectors were controlled by a spectrum stabilizer. Both scattering components were recorded simultaneously by a two-ADC multichannel analyzer. Radiation not emanating from the scatterer was determined by shifting the scatterer along the polarimeter axis out of the field of view of the detectors.

For symmetry considerations the recording system was entirely inverted at each run by turning the lead block which contains the detector slits and the scatterer (Fig. 3) and exchanging the detectors; the geometrical means of the pulse height distributions measured in both polarimeter positions for the parallel and the vertical scattering component were taken for further data analysis. To check for horizontal and vertical beam-line symmetry, measurements were taken at the photon emission angles $\theta = +10°$, $\theta = -10°$, and $\theta = 0°$.

III. DATA ANALYSIS

The measured pulse-height spectra had to be corrected for the response characteristics of the polarimeter, and the influence of elastic scattering of electrons in the target had to be eliminated.

A. Polarimeter response correction

In the case of an ideal polarimeter, with point scatterer and with point detectors of perfect ener-

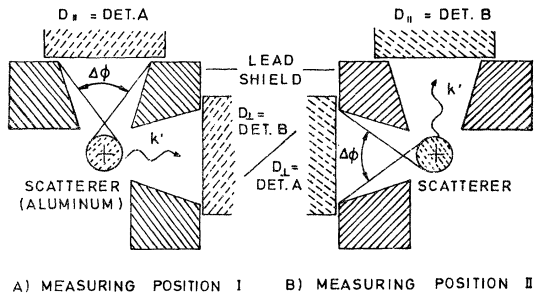

FIG. 3. Schematic cross sections of the Compton polarimeter. Detectors A and B (respectively, $D_{\parallel}$ and $D_{\perp}$) are scintillation detectors.

gy resolution, the bremsstrahlung polarization $P(k)$ for a given photon energy k might be easily derived from the measured pulse-height spectra as

$$P(k)=\frac{1}{S(k,\delta)}\,\frac{N_{\perp}(k')-N_{\parallel}(k')}{N_{\perp}(k')+N_{\parallel}(k')}\,. \tag{1}$$

$S(k,\delta)$ is the polarization sensitivity of the Compton process for the polarimeter scattering angle δ and the incident photon energy k (see Fig. 4), and $N_{\parallel}(k')$ and $N_{\perp}(k')$ are the numbers of scattered photons (energy k') recorded by detectors $D_{\parallel}$ and $D_{\perp}$, respectively (see Fig. 3). k is obtained from k' by the Compton energy relation

$$k=k'[1-k'(1-\cos\delta)/m_0c^2]^{-1}. \tag{2}$$

In the real polarimeter, finite solid angles are needed for efficiency, and consequently there is a certain energy interval $\Delta k'$ assigned to the scattered photons for a given incident energy k. When multiple scattering of photons in the scatterer is neglected, the energy response and the polarization sensitivity of the polarimeter can be calculated by numerical integration of the Klein-Nishina formula.[11] For the consideration of multiple scattering, comprehensive Monte Carlo calculations were made which are reported elsewhere (Lichtenberg and Przybylski[12]). The influence of multiple scattering on the polarization sensitivity is shown in Fig. 4.

The relation between the measured pulse-height distributions $M_i^{\parallel}$ and $M_i^{\perp}$ and the spectra of the (entirely polarized) bremsstrahlung components $C_j^{\parallel}$ and $C_j^{\perp}$ is described by the equations

$$M_i^{\parallel}=\sum_j (A_{ij}C_j^{\parallel}+B_{ij}C_j^{\perp}),$$
$$M_i^{\perp}=\sum_j (A_{ij}C_j^{\perp}+B_{ij}C_j^{\parallel}), \tag{3}$$

where A_{ij} and B_{ij} (each consisting of 64×64 elements) are the polarimeter response matrices. The columns of matrix A_{ij} represent the pulse-height distributions for scattering perpendicular to the plane of primary polarization, while B_{ij} describes parallel scattering. The matrices include the scintillation-detector response, which was determined in the usual way with a number of radioisotopes.

To obtain the bremsstrahlung components $C_j^{\parallel}$ and $C_j^{\perp}$ from $M_i^{\parallel}$ and $M_i^{\perp}$, the matrix equations (3) were solved iteratively in a similar way as described by Skarsgard, Johns, and Green[13] for a single spectrometer. Peculiarities arise from the fact that the two scattering components cannot be treated independently. Starting vectors $C_{i;0}^{\parallel}$ and $C_{i;0}^{\perp}$ for the iteration were obtained by assuming an ideal energy resolution of the polarimeter (S_i = polarization sensitivity for photons recorded in the ith channel)

$$\left.\begin{matrix}C_{i;0}^{\parallel}\\ C_{i;0}^{\perp}\end{matrix}\right\}=\tfrac{1}{2}(M_i^{\parallel}+M_i^{\perp})\pm(M_i^{\parallel}-M_i^{\perp})/2S_i\,. \tag{4}$$

For the further iteration, weighted corrections were derived from the differences between $M_i^{\parallel}$ and $M_i^{\perp}$ and the pulse-height distributions calculated according to formula (3) from the assumed bremsstrahlung components (for details see Lichtenberg[14]),

$$\left.\begin{matrix}C_{i;l+1}^{\parallel}\\ C_{i;l+1}^{\perp}\end{matrix}\right\}=\left\{\begin{matrix}C_{i;l}^{\parallel}\\ C_{i;l}^{\perp}\end{matrix}\right\}\times\Bigg(2-(1\mp S_i)\sum_j\frac{A_{ij}C_{j;l}^{\perp}+B_{ij}C_{j;l}^{\parallel}}{2M_i^{\perp}}-(1\pm S_i)\sum_j\frac{A_{ij}C_{j;l}^{\parallel}+B_{ij}C_{j;l}^{\perp}}{2M_i^{\parallel}}\Bigg)\,. \tag{5}$$

Starting the iteration procedure with pulse-height

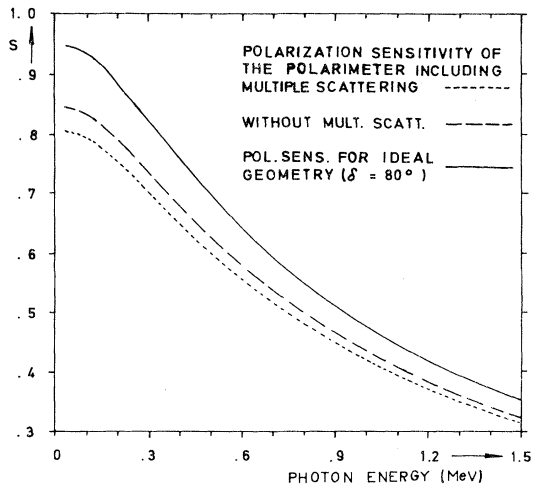

FIG. 4. Polarization sensitivity of the Compton elementary process, of the polarimeter for single scattering only and with consideration of multiple scattering.

distributions which are affected by counting statistics would lead to spectra with line structure. As the spectral distribution of bremsstrahlung is expected to be smooth (characteristic x rays were removed from the spectra by graphic interpolation in the case of gold targets), a least-squares fit with polynomials of the fourth order was first applied to the logarithms of the pulse-height distributions. The iteration was continued until the relative differences between the measured and the calculated distributions were less than 2.5×10^{-3}, requiring about 10 correction steps.

B. Influence of electron scattering

In the present work the influence of elastic scattering of electrons by target atoms on the degree of polarization measured was for the first time quantitatively taken into account. Electron scattering affects polarization in two ways: (a) It causes an uncertainty in photon emission angle, and (b) as the scattering is three-dimensional, the reaction plane generally makes an angle with the plane of observation. The latter effect has been neglected by other authors, probably because it is meaningless for total cross-section measurements, but it implies considerable error in polarization measurements, especially for small photon emission angles. One obtains, e.g., a relative error of 13% for a beryllium target 4.3 mg/cm^2 thick at $T_1=0.5$ MeV, $\theta=10°$, and $k/T_1=0.9$ (while Motz and Placious[4] expect a negligible effect), or a relative error of 7% for an aluminum target 50 μg/cm^2 thick at $T_1=50$ keV, $\theta=22.5°$, and $k/T_1=0.8$ [while Kuckuck and Ebert[15] expect an error of (0.5-2)%].

The polarization errors were calculated by convoluting electron scattering distributions (taken from the Keil, Zeitler, and Zinn[16] tables) and bremsstrahlung cross sections (computed in Born approximation with exponential screening according to Fronsdal and Überall[17]). In Fig. 5 angular relations are illustrated; the target is in the origin, and the incident electrons travel along the z axis. Bremsstrahlung is observed in the xz plane at an angle θ. If θ_e and ϕ_e denote the angles of electron scattering before bremsstrahlung production, the true photon emission angle θ_k is given by

$$\cos\theta_k=\sin\theta\sin\theta_e\cos\phi_e+\cos\theta\cos\theta_e\,, \tag{6}$$

and for the angle β between the reaction plane and the observation plane one obtains

$$\cos\beta=(\sin\theta\cos\theta_e-\sin\theta_e\cos\theta\cos\phi_e)/\sin\theta_k\,. \tag{7}$$

The relation between the intrinsic bremsstrahlung cross sections $d^2\sigma_\perp$ and $d^2\sigma_\parallel$ and the measured cross section $d^2\sigma_{\perp m}$ (in similar form for $d^2\sigma_{\parallel m}$) is given by the convolution integral

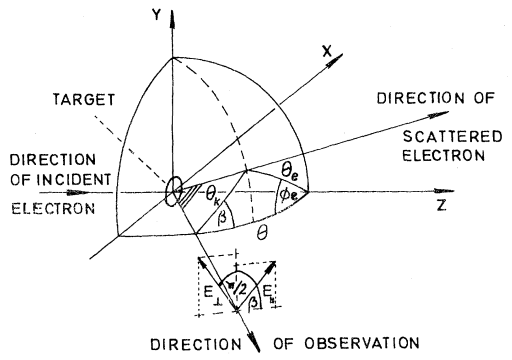

FIG. 5. Bremsstrahlung production by an elastically scattered electron.

$$d^2\sigma_{\perp m}(\theta)=\int_{\theta_e}F(\theta_e)\theta_e\int_{\phi_e}[d^2\sigma_\perp(\theta_k)\cos^2\beta+d^2\sigma_\parallel(\theta_k)\sin^2\beta]\,d\phi_e\,d\theta_e+Ud^2\sigma_\perp(\theta)\,. \tag{8}$$

$F(\theta_e)$ denotes the electron scattering distribution averaged over target thickness; U is the fraction of unscattered electrons. The integrals $d^2\sigma_{\perp m}$ and $d^2\sigma_{\parallel m}$ must be evaluated numerically.

The calculated influence of electron scattering on polarization was verified experimentally by runs with different target thicknesses. For the measurements we report, the targets were thin enough to limit the electron scattering correction to less than 10%; target thickness was individually selected for each electron energy, target Z, and photon angle. For the target thicknesses used, the effect of electron energy loss on polarization was calculated to be negligible.

C. Experimental errors

In addition to statistical uncertainty, known sources of systematic error are the following:

(a) Inaccuracy in electron energy $|\Delta T_1/T_1|<9\times10^{-3}$, resulting from (i) the width of the energy-defining slits (see Sec. II), (ii) the electron energy loss in the target, and (iii) electron energy calibration, which was performed by measuring the bremsstrahlung short-wavelength limit with a Ge(Li) spectrometer.

(b) Uncertainty in photon emission angle $|\Delta\theta|<0.35°$, mainly caused by the extension of the beam focus spot. The direction of the beam is horizontally defined to $\pm0.15°$; the vertical error of $\pm0.5°$ will affect the photon emission angle θ only negligibly.

(c) Error in spectral energy, $2.5\times10^{-3}<|\Delta k/T_1|<8\times10^{-3}$, due to channel width, calibration, and stability of the analyzer used. The error is greatest near the short-wavelength limit and lowest at

small k/T_1 because of the nonlinearity of the Compton energy relation.

(d) Limited accuracy of the polarimeter response correction, inducing a polarization error $|\Delta P| < 5\times10^{-3}$ (minimized by using two detectors simultaneously and rotating the polarimeter for symmetry, and by quantitative consideration of multiple scattering of photons). In the case of $T_1 = 0.533$ MeV, $k/T_1 < 0.2$, there is an additional error $|\Delta P| < 2\times10^{-3}$ due to iodine escape peaks.

(e) Uncertainty in the electron scattering correction, because of target inhomogeneity and the use of Born-approximation cross sections in the calculations, causing an error $|\Delta P/P| < 10^{-2}$. The polarization error $|\Delta P|$ induced by photon scattering in the collimator is less than 10^{-4}.

In the low-energy part of the spectrum systematic errors are predominant; for high photon energies statistical errors prevail (especially at large photon emission angles owing to noticeable contributions of background radiation). In Figs. 8–12 the error bars include systematic and statistical errors.

IV. RESULTS AND DISCUSSION

Bremsstrahlung polarization was measured for incident electron energies of 0.533, 1.0 and 1.5 MeV and photon emission angles of 10°, 20°, 30°, 40°, 60°, 90° (except for $T_1 = 1.5$ MeV) and 122.5° (only for $T_1 = 0.533$ MeV). Targets of gold ($Z = 79$), silver ($Z = 47$), aluminum ($Z = 13$), and, for emission angles of 10°–30°, beryllium ($Z = 4$) were used. In this paper only a selection of the experimental results can be presented (for complete results see Lichtenberg[14]).

A. Outline of theoretical predictions

The measurements are compared with Born approximation theory including screening (calculated according to Fronsdal and Überall[17]), with calculations using Sommerfeld-Maue eigenfunctions[18] (according to Haug[19]) and, where available, with partial-wave calculations (by Tseng and Pratt[8]). The three theories show no difference in bremsstrahlung linear polarization for low-Z targets, but for high Z the predictions are in remarkable disagreement.

In *Born approximation* theory (Bethe-Heitler formula[1]) the wave functions of free particles are used to describe the incident and the final electron, disregarding the influence of the atomic field. This is reasonable only if $Z/137\,\beta_0 \ll 1$ and $Z/137\,\beta \ll 1$, where β_0 and β are, respectively, the velocities of the incident and the final electron. For relativistic electron energies ($\beta_0 \approx 1$) both conditions are satisfied for low Z and photon energies not too close to the short-wavelength limit. Without consideration of screening there is no Z dependence of polarization in Born approximation.

Fronsdal and Überall[17] have calculated bremsstrahlung polarization on the basis of the Bethe-Heitler formula using exponential screening. The Z dependence of polarization due to screening is limited to small photon emission angles and to very low spectral energies k/T_1 (see Fig. 6).

In the theory of Elwert and Haug[5,6] bremsstrahlung is calculated using *Sommerfeld-Maue eigenfunctions*,[18] which are solutions of the Dirac equation in first order in $Z/137$; screening is neglected. The calculations should be valid for all spectral energies provided that $Z/137 \ll 1$, i.e., for low Z. From the Elwert-Haug theory, finite cross sections result for $k/T_1 \approx 1$, where Born approximation breaks down. The polarization data for low Z are nearly identical with the Born-approximation predictions, even where the cross sections differ strongly.

In order to demonstrate the Z dependence of polarization expected at an incident electron energy of 0.5 MeV, calculations for $Z = 4$ and $Z = 79$ are shown in Fig. 7 (obtained by numerical integration of an unpublished formula of Haug[19]). The curves for $Z = 4$ coincide with Born approximation data within a linewidth.

Tseng and Pratt[7,8] calculate the bremsstrahlung process by means of *partial-wave expansions*, using point Coulomb as well as screened potentials. Their results should apply to all target atomic numbers and to all spectral energies. For low-Z targets the calculations are compatible with Born

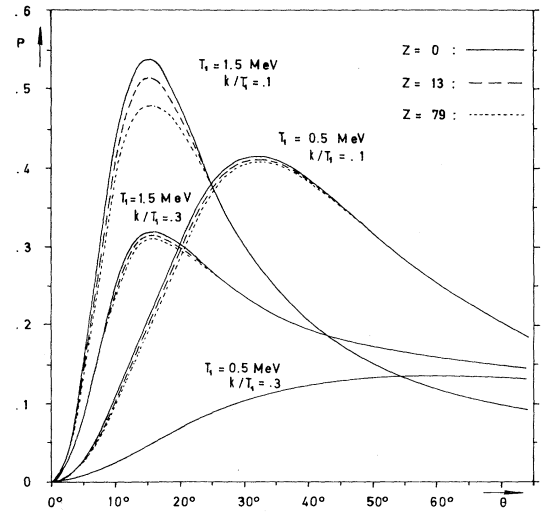

FIG. 6. Z dependence of polarization in Born approximation (due to screening), calculated according to Fronsdal and Überall (Ref. 17).

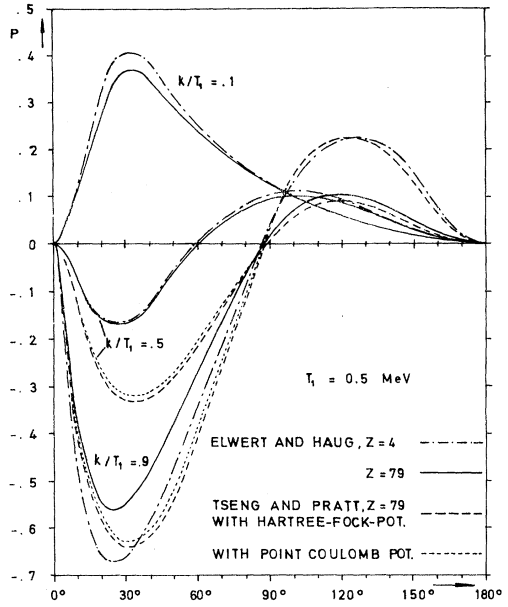

FIG. 7. Polarization predicted by Elwert and Haug theory (Ref. 19, for $Z=4$ and $Z=79$, $k/T_1=0.1$, 0.5, 0.9) and by partial-wave calculations (Ref. 8, for $Z=79$, $k/T_1=0.5$, 0.9). Incident electron energy $T_1=0.5$ MeV.

approximation theory as far as linear polarization is concerned.

For high Z the available results are plotted in Fig. 7. The degree of polarization obtained with point Coulomb potential and with a Hartree-Fock-Slater potential[7] for an electron energy of 0.5 MeV is shown. Most striking is the Z dependence observed at the photon energy $k/T_1=0.5$, where the Elwert-Haug calculations indicate nearly no effect of target atomic number. The choice of atomic potential is of little influence compared with the difference to the Elwert-Haug data and to Born approximation theory.

B. Results for low-Z targets

It turns out that for low-Z targets all the calculations discussed in the previous section describe the experimental results satisfactorily, as illustrated by Figs. 8 and 9.

Figure 8 presents polarization as a function of photon energy for incident electron energies of 0.533, 1.0, and 1.5 MeV and an emission angle $\theta=20°$, i.e., the region of maximum polarization. Solid lines are from Born approximation theory for low-Z targets. High-Z experimental results are included in this figure to give an idea of the magnitude of the Z influence to be observed across the spectrum. In Fig. 9 polarization is plotted as a function of photon emission angle with spectral energy k/T_1 as a parameter. The target material

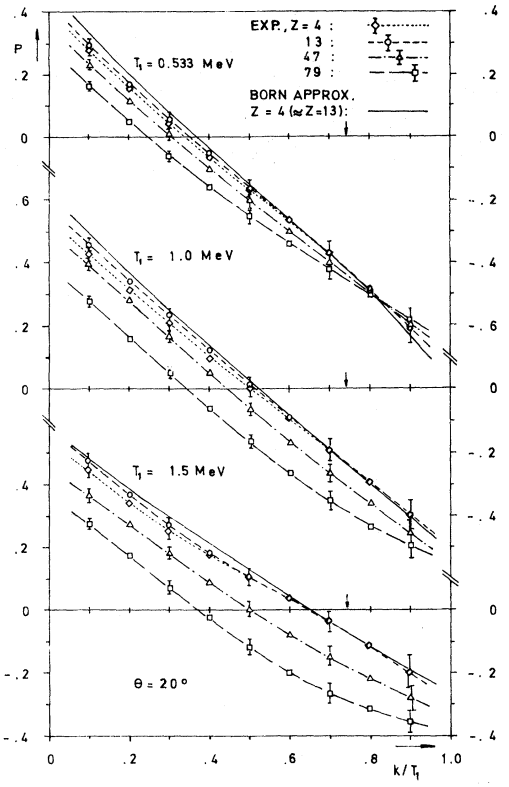

FIG. 8. Experimental results for different T_1 and Z and Born-approximation data (Ref. 17); the limit of electron-electron bremsstrahlung is marked by arrows, $\theta=20°$.

was aluminum, the incident electron energy 1.0 MeV. Solid lines are again calculated according to Fronsdal and Überall.[17]

The agreement of the low-Z measurements with

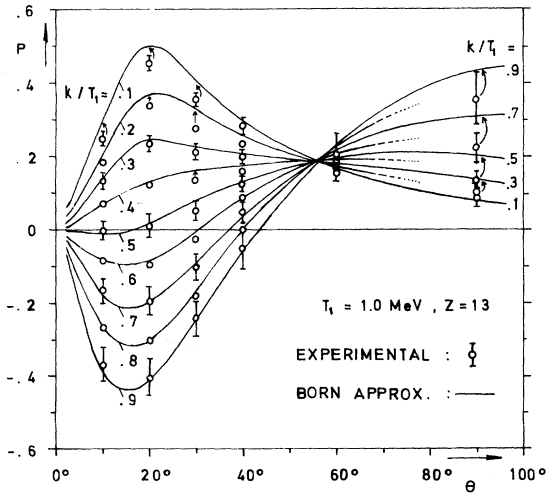

FIG. 9. Low-Z experimental results and calculations according to Fronsdal and Überall (Ref. 17, $T_1=1.0$ MeV, $Z=13$).

Born approximation theory holds even near the short-wavelength limit, where the predictions are expected to fail. The breakdown of the Born approximation in total cross sections does obviously not affect linear polarization, i.e., the components $d^2\sigma_\perp$ and $d^2\sigma_\parallel$ must be wrong by the same factor.

It should be noted that at low photon energies, where good agreement with Born approximation should be certain, slight differences between theory and experiment are observed. The polarization obtained with aluminum targets does not quite reach the theoretical values here, and, proceeding to the beryllium measurements, there is an inversion in Z dependence (Fig. 8). Target materials were sufficiently pure that this observation can only be explained by the inevitable contribution of electron-electron bremsstrahlung roughly increasing with $1/Z$ (see, e.g., Achieser and Berestezki[20]). This is supported by the fact that the differences do not go beyond the short-wavelength limit of electron-electron bremsstrahlung (lower than that of nuclear bremsstrahlung due to kinematics). There are no theoretical predictions on electron-electron bremsstrahlung polarization at present; the measurements indicate that it should have a very low degree of polarization at photon emission angles of 20°–30°.

The quantitative proof of Born approximation theory for low-Z targets had been left open to question by other authors. The early polarization experiments of Motz and Placious[4] at incident electron energies of 0.5 and 1.0 MeV and spectral energies $k/T_1 = 0.1$ and 0.9 show agreement with theoretical predictions only for intermediate photon emission angles. The more recent measurements of Rank and Unfried[21] (at $T_1 = 2$ MeV)

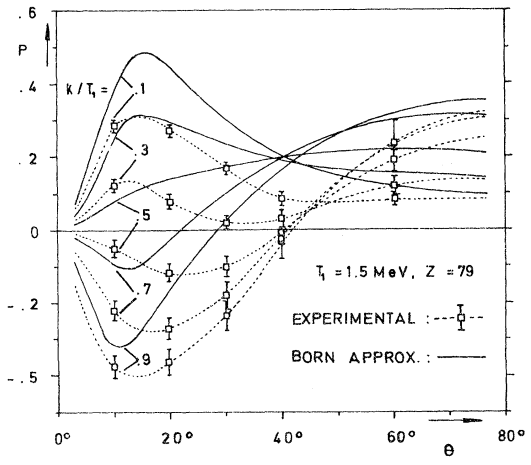

FIG. 10. High-Z experimental results and calculations according to Fronsdal and Überall (Ref. 17, $T_1 = 1.5$ MeV, $Z = 79$).

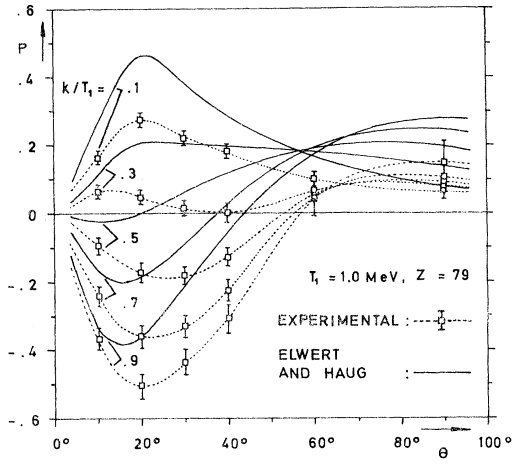

FIG. 11. Experimental results and Elwert-Haug data (Ref. 19) for $Z = 79$, $T_1 = 1.0$ MeV.

and of Kuckuck and Ebert[15] (at $T_1 = 50$, 75, and 100 keV) also differ from Born approximation theory, especially for small photon emission angles. All these experimental results were obtained neglecting the effects of electron scattering and multiple photon scattering (Sec. III).

C. Results for high-Z targets

In the case of high-Z targets the experimental data agree only with the partial-wave calculations of Tseng and Pratt[8]; Born approximation theory[17] and the Elwert-Haug calculations[19] are likewise inconsistent with the measurements. This is illustrated in Figs. 10–12. In Fig. 10 the polarization observed with gold targets is compared with Born approximation theory (incident electron energy

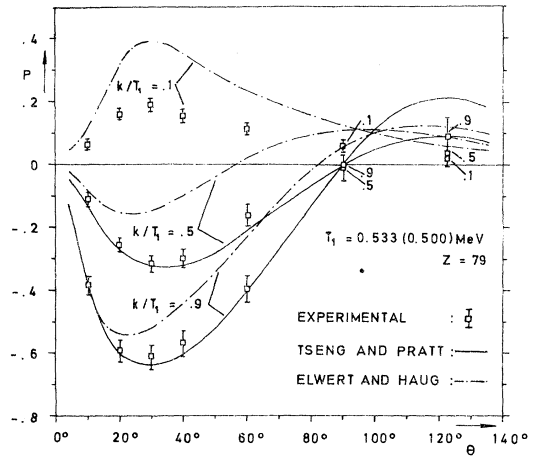

FIG. 12. Experimental results ($T_1 = 0.533$ MeV) and data from Tseng and Pratt (Ref. 8, $T_1 = 0.500$ MeV, Hartree-Fock-Slater potential) and Elwert and Haug (Ref. 19, $T_1 = 0.533$ MeV); $Z = 79$.

1.5 MeV). In Fig. 11 a comparison of gold target measurements at an electron energy $T_1 = 1.0$ MeV with Elwert-Haug data is shown. Figure 12 indicates the validity of the partial-wave results of Tseng and Pratt available for high-Z targets.

It is not surprising that the Born-approximation data are poor for high-Z measurements (see Sec. IV A). The Elwert-Haug calculations also fail to explain the strong Z dependence observed (Fig. 11). Our measurements with silver targets likewise differ from the data of both theories. For the Elwert-Haug calculations, the discrepancies become smaller with decreasing electron energy. The calculations are in satisfactory agreement with high-Z experimental data at still lower electron energies, e.g., $T_1 = 180$ keV (see Scheer, Trott, and Zahs[22]). In the electron energy range of 0.5–1.5 MeV, however, the Elwert-Haug polarization results seem to have little more validity than Born approximation theory.

The agreement with the Tseng and Pratt data (Fig. 12) is very good for emission angles $\theta \leq 90°$; slight differences are partly due to dissimilar incident electron energies (0.533 MeV for the measurements and 0.500 MeV for the calculations). Elwert-Haug theory (dotted lines) seems to be acceptable for the angle $\theta = 122.5°$ here. It would be very instructive to have a more complete comparison of the experimental results with partial-wave calculations, but unfortunately there are no more data of this kind available at present.

The experimental results of Motz[23] obtained with a gold target for an incident electron energy $T_1 = 1$ MeV and a photon emission angle $\theta = 20°$ are in agreement with the present work (Fig. 8). The angular dependence of polarization measured by Motz and Placious[4] with gold targets ($k/T_1 = 0.1$ and 0.9) is compatible with the present data at $T_1 = 1$ MeV, except for $\theta = 90°$, whereas comparison at $T_1 = 0.5$ MeV is less favorable.

ACKNOWLEDGMENTS

The authors are grateful to Dr. E. Haug for providing unpublished theoretical results and would also like to thank Professor G. Elwert and Professor R. H. Pratt for interesting discussions.

[1] H. Bethe and W. Heitler, Proc. R. Soc. A 146, 83 (1934).
[2] P. Kirkpatrick and L. Wiedmann, Phys. Rev. 67, 321 (1945).
[3] H. Olsen and L. C. Maximon, Phys. Rev. 110, 589 (1958).
[4] J. W. Motz and R. C. Placious, Nuovo Cimento 15, 571 (1960).
[5] G. Elwert and E. Haug, Phys. Rev. 183, 90 (1969).
[6] E. Haug, Phys. Rev. 188, 63 (1969).
[7] H. K. Tseng and R. H. Pratt, Phys. Rev. A 3, 100 (1971).
[8] H. K. Tseng and R. H. Pratt, Phys. Rev. A 7, 1502 (1973).
[9] W. Järisch, thesis (Würzburg University, 1967) (unpublished).
[10] T. Nowak, thesis (Würzburg University, 1967) (unpublished).
[11] D. Klein and Y. Nishina, Z. Phys. 52, 853 (1929).
[12] W. Lichtenberg and A. Przybylski, Nucl. Instrum. Methods 98, 99 (1972).
[13] C. D. Skarsgard, H. E. Johns, and L. E. S. Green, Radiat. Res. 14, 261 (1961).
[14] W. Lichtenberg, thesis (Würzburg University, 1973) (unpublished).
[15] R. W. Kuckuck and P. J. Ebert, Phys. Rev. A 7, 456 (1973).
[16] E. Keil, E. Zeitler, and W. Zinn, Z. Naturforsch. A 15, 1031 (1960).
[17] C. Fronsdal and H. Überall, Phys. Rev. 111, 580 (1958).
[18] A. Sommerfeld and A. W. Maue, Ann. Phys. (Leipz.) 22, 629 (1935).
[19] E. Haug (private communication).
[20] A. I. Achieser and W. B. Berestezki, *Quantenelektrodynamik* (Teubner, Leipzig, 1962).
[21] D. Rank and E. Unfried, Z. Phys. 233, 231 (1970).
[22] M. Scheer, E. Trott and G. Zahs, Z. Phys. 209, 68 (1968).
[23] J. W. Motz, Phys. Rev. 104, 557 (1956).